HHS Public Access

Author manuscript

ACS Appl Mater Interfaces. Author manuscript; available in PMC 2017 March 16.

Published in final edited form as:

ACS Appl Mater Interfaces. 2016 March 16; 8(10): 6320–6328. doi:10.1021/acsami.5b10883.

An Approach to Rapid Synthesis and Functionalization of Iron Oxide Nanoparticles for High Gene Transfection

Zachary R. Stephen[1], **Christopher J. Dayringer**[1], **Josh J. Lim**[1], **Richard A. Revia**[1], **Mackenzie V. Halbert**[1], **Mike Jeon**[1], **Arvind Bakthavatsalam**[2], **Richard G. Ellenbogen**[3,4], and **Miqin Zhang**[1,3,*]

[1]Department of Materials Science and Engineering, University of Washington, Seattle, Washington 98195

[2]Department of Biochemistry, University of Washington, Seattle, Washington 98195

[3]Department of Neurological Surgery, University of Washington, Seattle, Washington 98195

[4]Department of Radiology, University of Washington, Seattle, Washington 98195

Abstract

Surface functionalization of theranostic nanoparticles (NPs) typically relies on lengthy, aqueous post-synthesis labeling chemistries that have limited ability to fine tune surface properties and can lead to NP heterogeneity. The need for a rapid, simple synthesis approach that can provide great control over the display of functional moieties on NP surfaces has led to increased use of highly selective bioorthoganol chemistries including metal-affinity coordination. Here we report a simple approach for rapid production of a superparamagnetic iron oxide NPs (SPIONs) with tunable functionality and high reproducibility under aqueous conditions. We utilize the high affinity complex formed between catechol and $Fe^{(III)}$ as a means to dock well-defined catechol modified polymer modules on the surface of SPIONs during sonochemical co-precipitation synthesis. Polymer modules consisted of chitosan and poly(ethylene glycol) (PEG) copolymer (CP) modified with catechol (CCP), and CCP functionalized with cationic polyethylenimine (CCP-PEI) to facilitate binding and delivery of DNA for gene therapy. This rapid synthesis/functionalization approach provided excellent control over the extent of PEI labeling, improved SPION magnetic resonance imaging (MRI) contrast enhancement and produced an efficient transfection agent.

Abstract

*Miqin Zhang, Department of Materials Science & Engineering, University of Washington, mzhang@uw.edu, 302L Roberts Hall, Box 352120, Seattle, WA 98195, Fax: (206) 543-3100.

Supporting Information. Supporting methods, chemical schematics of polymer synthesis, evaluation of Cy5 loading, TEM characterization of SPION core size and morphology, SAED analysis of SPION lattice structure, VSM analysis of SPION magnetic properties, optimization of DNA complex ratios and optimization of DNA treatment dose for *in vitro* transfections. This material is available free of charge *via* the internet at http://pubs.acs.org.

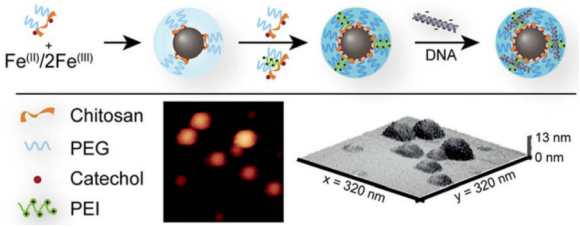

Keywords

Iron oxide; nanomaterials; gene therapy; theranostics; cancer

INTRODUCTION

Theranostic NPs capable of diagnostic imaging and therapeutic drug delivery have potential to revolutionize current clinical approaches to cancer therapy.[1–5] Of the nanomaterials studied to this end, iron oxide nanoparticles have emerged as one of top candidates. Their intrinsic superparamagnetism enables non-invasive MRI, and their biodegradability is advantageous for *in vivo* applications.[2, 6–7] The successful translation of theranostic NPs to clinic will require the development of simplified production processes that lead to reproducible NPs with control over surface functionality while maintaining excellent imaging sensitivity. However, theranostic NPs are inherently complex, typically containing endogenous and/or exogenous imaging components, therapeutic agent(s), and targeting ligands with each component typically added through time consuming multi-step processes (i.e., each step involving processes such as surface modification, characterization, and purification). Unlike polymer conjugates, theranostic SPION conjugates are generally difficult to characterize because their nanosized feature and magnetic properties cause fluorescence quenching and NMR peak broadening and inconsistencies in peak ratios.[8] More importantly, post synthesis surface modification of theranostic SPIONs (and other NPs as well) relies primarily on aqueous chemistries that are prone to hydrolysis and unwanted crosslinking, and often lacks reaction site specificity,[9] yielding limited ability to fine tune surface functionality and maintain batch-to-batch consistency. Furthermore, surface coatings produced by existing methods would more or less reduce the intrinsic magnetism of SPIONs.

The complex formed between catechol and $Fe^{(III)}$ is extremely stable due to the σ- and π-donor bond contributions[10] and researchers have previously exploited the $Fe^{(III)}$-catechol interaction to yield ultra-stable catechol-polymer capped SPIONs with improved magnetic properties.[11–16] However, to date, all catechol-polymer capped SPIONs have been produced through laborious ligand exchange processes subsequent to SPION synthesis, typically by the thermal decomposition method. The thermal decomposition synthesis of SPIONs requires one day to produce an Fe-oleate complex followed by a second day to thermally decompose the Fe-oleate complex and purify the product to produce water-insoluble oleic acid coated SPIONs that must then undergo ligand exchange process to infer water solubility. In addition, biomedical application of SPIONs normally requires additional

chemistry to enable appropriate surface functionality, which requires additional processing time (days).

Here we report a simple method for production of a SPION gene transfection agent utilizing polymer modules consisting of chitosan and poly(ethylene glycol) (PEG) copolymer (CP) modified with catechol (CCP), and polyethylenimine (PEI) modified CCP (CCP-PEI) that exhibit high affinity and specificity for iron oxide surfaces. Utilization of an aqueous sonochemical co-precipitation synthesis method under ultrasonic irradiation modified by reducing polymer concentration during initial synthesis and addition of functionalized polymer post-synthesis, facilitated a rapid synthesis/coating/functionalization of theranostic SPIONs. Sonochemical co-precipitation has proven to be a useful method for synthesis of iron oxide nanoparticles.[17–18] Ultrasonic irradiation can enhance chemical reactions through acoustic cavitation that produce collapsing bubbles in liquid media that generate high local temperature and pressure pulses and serve as microreactor hot spots.[19] The subsequent temperature and pressure gradients also create a mechanical stirring effect and provide rapid mixing of the reaction solution to minimize pH gradients during co-precipitation. The high affinity of the catechol functionalized polymer for the iron oxide core provided the ability to fine-tune important physiochemical properties by altering feed ratios of the polymer modules which improved reproducibility through strong site-specific interaction between the iron oxide core and catechol-functionalized polymer coating and increased MR relaxivity in comparison to non-catechol-capped SPIONs.

As a model system, PEI was chosen as a CCP modifier to infer functionality through its cationic charge capable of efficiently binding DNA for gene therapy applications. However, we anticipate this approach to be widely applicable to other therapeutic platforms by simply replacing PEI modified CCP with a suite of chemo/biotherapeutic and targeting ligand modified CCP to allow a highly customizable approach to patient care. Our approach directly produces water-soluble, catechol capped SPIONs with appropriate surface functionality for gene delivery in less than 24 h including ~2 h of active time and an overnight aging step. Furthermore, our simplified approach significantly reduces the batch-to-batch variation, which is normally proportional to the chemical reaction steps involved.

MATERIALS AND METHODS

Materials

All reagents were purchased from Sigma-Aldrich (St. Louis, MO) unless otherwise specified. The low molecular weight chitosan was purchased from Acemey Industrial (Shanghai, China). The heterobifunctional linker 2-iminothiolane (Traut's reagent) and succinimidyl iodoacetate (SIA) was purchased from Molecular Biosciences (Boulder, CO). NHS-PEG_{12}-maleimide was purchased from Thermo Fisher Scientific (Rockford, IL). Tissue culture reagents including DMEM and antibiotic-antimycotic were purchased from Invitrogen (Carlsbad, CA). Fetal bovine serum (FBS) was purchased from Atlanta Biologicals (Lawrenceville, GA).

Polymer synthesis

2,300 MW chitosan oligosaccharide (1.3 mmol) was dissolved in 40 mL DI water and 8 mL methanol was added drop-wise and the solution was pH was adjusted to 6.5. Aldehyde-activated methoxy PEG (13 mmol) produced by the Pfitzner-Moffatt oxidation of 2000 MW methoxy-PEG-OH, and 3,4-dihydroxybenzaldehyde (5.2 mmol, DHBA) dissolved in 16 mL DI water were then added drop-wise and reacted for 1 h. 1.0 M sodium cyanoborohydride (185 μL, diluted to 12 mL in DI water) was added drop-wise and the solution was reacted for an additional 18 h. The resulting catechol functionalized chitosan-PEG (CCP) was precipitated with acetone, collected with a Buchner funnel, washed three times with acetone to remove unreacted PEG, dried by vacuum, redispersed in DI water and further purified by tangential flow filtration (TFF, Millipore, Billerica, MA) using a 5 k MW cutoff cassette. The purified polymers were freeze-dried and stored at −20 °C.

CCP was further modified with PEI (CCP-PEI) as follows: CCP (500mg) was dissolved at 100mg mL^{-1} in 0.1 M Na bicarbonate, 5 mM EDTA buffer at pH 8.0 and reacted with SIA (142 mg) dissolved in 1 mL dimethyl sulfoxide (DMSO) and reacted for 1 h at room temperature with gentle rocking. Simultaneously, 6.25 g of 25 k MW PEI was dissolved in 20 mL 0.1 M Na bicarbonate, 5 mM EDTA bufferr at pH 8.0, and Traut's reagent (40 mg at 10mg mL^{-1} in 0.1 M Na bicarbonate, 5 mM EDTA bufferr at pH 8.0) was added and reacted for 1 h at room temperature. SIA modified chitosan and Traut's reagent modified PEI were added together and reacted for 30 m. The CCP-PEI reaction mixture was purified by dialysis against DI water using 50 kDa MWCO Spectra/Por dialysis membrane (Spectrum Laboratories, Rancho Dominguez, CA). The purified polymers were freeze-dried and stored at −20 °C.

CCP-Cy5 was synthesized as follows: 2.5 mg of Cy5-NHS ester (Lumiprobe, Hallandale, FL) was dissolved in 100 μL of anhhdrous DMSO and added to 35mg of CPP dissolved in 2 mL of anhydrous DMSO. 0.1% N,N-diisopropylethylamine was added as a base catalyst. The mixture was reacted for 48 h at room temperature and purified by dialysis against DI water using 8 kDa MWCO Spectra/Por dialysis membrane (Spectrum Laboratories, Rancho Dominguez, CA). Purified CCP was freeze-dried and stored at −20 °C.

NMR analysis

Polymer samples were prepared by dissolving polymer and TSP in D_2O and NMR spectra were obtained using a Bruker Avance 300 spectrometer operating at 300 MHz (^1H) and 298 K (number of scans = 64, acquisition time = 3.9 s, delay (D1) = 2 s).

Peak identification:

CP (PEG): ^1H NMR (300MHz, D_2O) δ 3.38 (3H, s)

CCP (catechol group): ^1H NMR (300MHz, D_2O) δ 7.1–6.75 (3H, m), 3.38 (3H, s)

CCP-PEI (PEI): ^1H NMR (300MHz, D_2O) δ 2.9–2.5

IOCCP and IOCCP-PEI synthesis

Iron oxide nanoparticles coated with CCP or CCP/CCP-PEI were synthesized *via* a sonochemical co-precipitation of iron chlorides in aqueous solution. Briefly, pure CCP (25 mg) was mixed with iron chlorides (9 mg $Fe^{(II)}$, 18 mg $Fe^{(III)}$) in 2.18 mL of degassed DI water. A 14.5 M solution of ammonium hydroxide was titrated in slowly at 40 °C with sonication (40 kHz, 110 W) provided by a Branson ultrasonic bath (Danbury, CT) until a final pH of 10.5 was reached to ensure nucleation of SPIONs. Upon completion of base titration, sonication was continued until a pH of 8.5–9.5 was reached due to evaporation of ammonia from the solution. For a typical synthesis, titration occurs concurrent to sonication over ~30 minutes with sonication continuing for ~10 minutes post titration. The total sonication time is held constant at 40 minutes. 50mg of additional polymer (CCP, or CCP/CCP-PEI) was then added and the SPIONs were incubated overnight at 4 °C. The synthesized IOCCPs/IOCCP-PEI were purified first by centrifugation at 3500 rcf for 10 minutes and the supernatant was further purified using size exclusion chromatography in S-200 resin (GE Healthcare, Piscataway, NJ) into 20 mM HEPES buffer, pH 7.4. IOCCP-Cy5 was synthesized in the same manner with CCP-Cy5 replacing CCP-PEI.

Hydrodynamic size and ζ potential characterization

Hydrodynamic size and ζ potential of IOCCP, IOCCP-PEI, and IOCCP-PEI complexed with DNA as described below was analyzed at 100 μg mL–1 in 20 mM HEPES buffer (pH 7.4) using a DTS Zetasizer Nano (Malvern Instruments, Worcestershire, UK).

TGA analysis

SPIONs were purified in to DI H_2O, freeze-dried, and ground into powder using a mortar and pestle. 3.5 ± 0.2 mg of SPION powder was placed in a platinum crucible and analyzed with a TGA Q50 system (TA Instruments, New Castle, DE) by ramping temperature at 20 °C/minute with a starting temperature of 25 °C and a final Temperature of 500 °C.

AFM analysis

IOCCP and IOCCP-PEI AFM samples were prepared by dropping and air-drying ~5 μg/mL of SPION solution in water on freshly cleaved mica. SPIONs images were acquired with a Dimension-3100 (Veeco/DI/Bruker, Madison, WI) in tapping mode in air with an antimony-doped silicon cantilever (FESP, Bruker, Madison, WI). The cantilever had a nominal spring constant of 2.8 N/m, a resonant frequency of 75 kHz, a length of 225 μm, and a tip radius of 8 nm. Images were processed using Gwyddion software.

MR relaxivity characterization of IOCCP and IOCCP-PEI

R_2 relaxivity ($1/T_2$) of SPIONs at concentrations of 0, 5, 10, 15, 20, and 25 μg Fe mL^{-1} in phosphate buffered saline was evaluated by MRI using a Bruker (Billerica, MA) 14 Tesla vertical-bore imaging system (Utlrashield 600 WB Plus) through multi-spin echo acquisitions. Glass vials (3.25 mm I.D., 5 mm O.D., 200 μL volume) were filled with 150 μL of SPION/PBS solution. The vials were secured and surrounded by water to serve as a homogeneous background signal to minimize magnetic susceptibility variations around the samples. The fixed samples were positioned in a 25 mm single-channel ^1H radiofrequency

receive coil (PB Micro 2.5). The samples were scanned with a quantitative T2 multi-spin multi echo scan sequence (MSME) (TR = 2500 ms, TE = 6.7 + 6n ms, [n=0–16], in-plane resolution 78×156 μm^2, matrix 256×128) with 0.5 mm slice thickness for 14 slices. Analysis of MRI data was accomplished with the FMRIB software library (FSL), Paravision 5.1 analysis package (Bruker), Osirix (Pixmeo), and ImageJ (NIH). T2 values were determined within a circular, 100-voxel region of interest.

PEGylation of IOCCP-PEI complexed with DNA

IOCCP-PEI complexed with DNA at a 10:1 w/w ratio of SPION to DNA was reacted with $SM(PEG)_{12}$ at 216 μg of $SM(PEG)_{12}$ per mg Fe in the dark with gentle rocking for 30 min. The $SM(PEG)_{12}$ modified IOCCP-PEI (IOCCP-PEI-PEG) was then purified using size exclusion chromatography in S-200 resin equilibrated with 20mM HEPEs, pH 7.4, and stored at 4 °C.

Cell Culture

SF767 human glioblastoma multiforme (GBM) cells (American Type Culture Collection, Manassas, VA) were cultured in DMEM supplemented with 10% FBS and 1% antibiotic-antimycotic (Invitrogen, Carlsbad, CA). Cultures were maintained at 37°C in a humidified incubator with 5% CO_2.

Cell viability assay

A cell viability assay using alamarBlue reagent (Invitrogen, Carlsbad, CA) was performed on Human GBM cell line SF767. Briefly, 96-well plates were inoculated with 5,000 cells per 100 μL of supplemented media and incubated overnight at 37°C in 95%/5% air/CO_2. Before treatment each well was increased in volume to 200 μL. Cells received treatments of SPION/DNA complex (10:1 w/w), PEI/DNA (10:1 w/w) or Lipofectamine 2000/DNA (3:1, w/w) prepared according to the manufacturer's instructions, and diluted to achieve 0.1, 0.5, 1, 2, 3, or 4 μg mL^{-1} DNA final concentration. Cells were incubated for 48 h with the transfection agents. Alamar blue reagent was added and incubated for 2 h according to manufacturer's instructions. Viability was quantified by fluorescence spectrophotometery using a fluorescence excitation wavelength of 550ex/590em on a SpectraMax i3 microplate reader (Molecular Devices, Sunnyvale, CA).

Confocal imaging

For each transfection condition, 50,000 SF767 cells were seeded onto 24 mm glass cover slips 12–16 h prior to transfection. Cells were transfected as described above, then 48 h after transfection, were washed thrice with PBS and fixed with 4% formaldehyde (methanol free, Polysciences Inc., Warrington, PA) in PBS for 30 minutes at room temperature. Fixative was then removed and cells were washed thrice with PBS to remove the formaldehyde. Cells were membrane-stained with WGA-AF647 (Invitrogen, Carlsbad, CA) according to the manufacturer's instructions. The slides were mounted using ProLong Gold antifade solution containing DAPI (Invitrogen, Carlsbad, CA) and imaged using a Nikon Eclipse TE2000s confocal fluorescence microscope (Nikon, Tokyo, Japan).

Cell transfections and flow cytometry analysis

Human GBM cell line SF767 was used to compare the transfection efficiency of the SPION formulations against a Lipofectamine 2000 standard (Invitrogen, Carlsbad, CA) and 25 K PEI using pRFP. Briefly, cells were seeded at 100,000 cells/well in 24-well plates 16 h prior to transfection. SPION/DNA complexes prepared at different ratios (w/w) as described above were added to 1 ml of fully supplemented culture media to give a final DNA concentration of 1 or 2 μg DNA mL^{-1} in each well and gently rocked to mix. Cells were incubated with complexes for 48 h. Transfections using the commercial agent, Lipofectamine 2000, were performed following the manufacturer's protocol. Visual confirmation of RFP transfection was obtained by confocal microscopy using 561 nm excitation. Quantitative transfection efficiency was collected by flow cytometry.

Cells were washed three times with PBS, and detached using TrypLE Express (Invitrogen, Carlsbad, CA), and suspended in PBS containing 2% FBS. 5,000 cells were then analyzed using a BD FACSCanto flow cytometer (Beckton Dickinson, Franklin Lakes, NJ) and data analyses were performed using the FlowJo software package (Tree Star, Ashland, OR).

Statistical analysis

Experiments were performed in triplicate and the data was statistically analyzed to express the mean ± standard deviation (SD) unless otherwise stated.

RESULTS AND DISCUSSION

Synthesis and characterization of CCP and CCP-PEI

The multi-dentate catechol polymers were synthesized by modification of low molecular weight chitosan (2300 MW) with aldehyde functionalized methoxy-PEG (mPEG-aldehyde, 2000 MW) and catechol analog 3,4-dihydroxybenzaldehyde (DHBA) through reductive amination (Figure 1a). PEI modified CCP (IOCCP-PEI, Figure 1b) was produced by coupling thiolated 25k MW PEI with iodoacetyl modified CCP (Scheme S1 in Supporting Information). The presence of catechol, PEG, and PEI on the chitosan backbone of CP (control), CCP and CCP-PEI were verified by ^{1}H-NMR (Figure 1c). Analysis of CCP showed the characteristic ^{1}H-NMR peak for the methoxy group of PEG present at $\delta = 3.38$ and the peaks corresponding to the catechol aromatic hydrogens were present at $\delta = 6.91–7.55$. The extent of grafting was calculated to be ~3 PEG/chitosan and ~2 catechol/chitosan (Equation S1 in Supporting Information) and CCP-PEI was 72% w/w PEI based on the characteristic ^{1}H-NMR peaks associated with ethylenimine ($-NH_2-CH_2-CH_2-$) in the CCP-PEI spectra. Adequate PEG grafting provides steric stabilization for NPs coated with CCP and moderates charge associated toxicity for PEI modified SPIONs.[20] The presence of multiple catechol groups on the chitosan backbone increases the affinity of polymer to the iron oxide core due to the multi-dentate effect.[21]

Synthesis and characterization of IOCCP and IOCCP-PEI

SPION synthesis by sonochemical co-precipitation of iron chlorides was carried out in the presence of low concentration CCP to produce a diffusely coated SPION (Intermediate IOCCP, Figure 2a). $Fe^{(II/III)}$ was precipitated from supersaturation by addition of ammonium

hydroxide in an ultrasound assisted environment. The ultrasonic irradiation provided rapid mixing, which minimizes pH gradients within the reaction mixture to facilitate homogenous nucleation and reduce the size dispersity of the synthesized SPIONs. This initial step was followed by the addition of CCP to produce chitosan-PEG coated SPIONs (IOCCP) or various ratios of CCP and CCP-PEI to produce PEI functionalized SPIONs (IOCCP-PEI) for gene delivery (Figure 2b). The cationic charge of PEI allows for efficient binding of DNA through electrostatic interaction with the negatively charged phosphate backbone (Figure 2c). An advantage of performing SPION synthesis in the presence of catechol-functionalized polymer is the avoidance of ligand exchange processes that can have deleterious effects on SPIONs magnetic properties due to incomplete ligand exchange.[22] The lack of competition for the SPION surface ensures unhindered catechol-iron interactions (Figure 2d).

To determine the best ratio of CCP to CCP-PEI for gene delivery applications, ζ potential measurements of IOCCP-PEI produced at various polymer ratios were evaluated to optimize cationic surface charge to be between 15-20 mV based on our previous experience with similar SPIONs.[23] The surface charge of IOCCP-PEI was found to be highly tunable and repeatable from batch to batch with the modular addition of CCP-PEI (Figure 3a). SPIONs synthesized with polymer modules consisting of CCP modified with Cy5 fluorophore (CCP-Cy5) were also highly tunable and repeatable in regards to fluorescent signal (Figure S1 in Supporting Information). IOCCP had a ζ potential of 5.8 ± 3 mV and increased to 21.2 ± 0.9 mV at 75% w/w feed ratio of CCP-PEI. Both the 25% CCP-PEI (17.3 ± 1.4 mV) and 50% CCP-PEI (19.9 ± 0.6 mV) ratio produced IOCCP-PEIs with ζ potentials in the 15-20 mV range, which warranted further screening of these two ratios in vitro. Pilot transfections studies indicated that the 50% w/w CCP-PEI ratio produced a far more efficient transfection agent than the 25% w/w CCP-PEI ratio (Figure S2 in Supporting Information). For the remainder of this article, all references to IOCCP-PEI refer to those synthesized with 50% w/w CCP-PEI unless otherwise stated. A comparison of the ζ potential distributions of IOCCP and IOCCP-PEI at the 50% w/w ratio of CCP-PEI to CCP is shown in Figure 3b.

Hydrodynamic size is a primary factor in determining the *in vivo* fate of NPs, affecting uptake, retention and clearance.[24–25] IOCCP and IOCCP-PEI had an average hydrodynamic size of 35 ± 2 nm and 72 ± 3 nm, respectively, which falls well within the appropriate range for navigation and evasion of the mononuclear phagocyte system (Figure 3c).[25] The increase in hydrodynamic size is likely due to the addition of relatively bulky PEI and increased organization of water along the polymer/water interface due to the high positive charge associated with PEI.

Thermal gravimetric analysis (TGA) was used to measure % weight loss to compare the polymer coating densities of the initial diffusely coated intermediate IOCCP, IOCCP, and IOCCP-PEI (Figure 3d). Since all SPIONs have a similar core diameter and iron oxide won't degrade at the evaluated temperatures, any differences in % weight loss are indicative of the density of the polymer surface coating. IOCCP showed a 20 % increase in % weight loss over intermediate IOCCP (dashed black arrows). IOCCP-PEI had an additional 18 % increase in weight loss compared to IOCCP (black arrows). The increase in polymer density for IOCCP-PEI is likely caused by the addition of highly branched PEI.

Despite differences in hydrodynamic size, TEM analysis of IOCCP and IOCCP-PEI showed no marked difference in core morphology or size (Figure S3a–d in Supporting Information). IOCCP and IOCCP-PEI iron oxide cores had a roughly spherical shape and size distribution analysis revealed similar average core diameters of 5.2 ± 1.4 nm and 5.3 ± 1.7 nm for IOCCP and IOCCP-PEI, respectively. Similar size and morphology is expected since SPION core nucleation and growth phases were completed before additional CCP or CCP/CCP-PEI was added to increase the polymer surface density. Structural information of IOCCP and IOCCP-PEI was obtained by selected area electron diffraction (SAED, Figure S4a–b in Supporting Information). Table S1 shows that the measured lattice spacing based on diffraction rings is in agreeance with the known lattice spacing for bulk Fe_3O_4. The diffraction rings indicate the samples are polycrystalline and the corresponding indices are indicative of the lattice facets of cubic magnetite.[26]

Atomic force microscopy (AFM) analysis provided size and morphology information of the non-hydrated polymer coated SPIONs (Figure 4a–d). IOCCP and IOCCP-PEI samples were prepared on a mica substrate and imaged in tapping mode. The spherical morphology is evident and the size in the x and y-planes is slightly smaller than the hydrodynamic size, which is expected given the lack of an associated water layer and subsequent drying effects. SPION height in the z-plane is less than that in the xy-plane most likely due to the collapse of the non-hydrated, highly flexible polymer coating and the affinity of the highly anionic mica substrate to the cationic polymer coatings.

Surface stabilization of SPIONs is necessary for in vivo applications, yet it is important that appropriate capping ligands capable of preserving or enhancing magnetic properties are chosen.[27–28] A major advantage to capping SPIONs with catechol-functionalized polymers is the improved magnetic properties,[29] which increases T2 contrast enhancement in MR imaging. SPIONs have a large proportion of under-coordinated atoms on the particle surface due to the large surface-area-to-volume ratio inherent to particles at this size. In addition, NPs have high curvature due to small particle radii resulting in canted spins and spin-glass-like behavior on the surface layer. These phenomena produce a magnetic dead surface layer[30–31] that reduce the magnetic diameter and the overall mass magnetization of SPIONs as compared to bulk magnetite, thereby reducing MR contrast enhancement. Catechol moieties, facilitated by their electron withdrawing structure, have shown to display spin-ordering behavior by satisfying under-coordinated $Fe^{(III)}$ atoms on SPION surfaces, rejuvenating the magnetic dead layer, producing a nonzero moment on the SPION surface, and drastically increasing magnetic susceptibility.[32] The magnetic behavior of IOCCP and IOCCP-PEI were investigated by vibrating sample magnetometry (Figure S5a–d, in Supporting Information). The magnetic hysteresis curves at room temperature indicate near zero coercivity, which is a characteristic property of superparamagnetic particles. Both IOCCP and IOCCP-PEI demonstrated high saturation magnetization of 63.1 and 51.7 emu/g Fe, respectively.

A comparison of MR R_2 relaxivity ($1/T_2$) for IOCCP-PEI and IOCCP at field strength of 14 T reveals similar R_2 values of 85.7 and 82.6 $s^{-1}mM^{-1}$, respectively (Figure 5a–b). The effect of catechol capping is well demonstrated by comparing R_2 values for IOCCP-PEI and IOCCP with the R_2 value for a similar polymer coated SPION measured at the same field

strength but with no catechol capping. CP coated SPIONs (IOCP) had a nearly 2-fold decrease in relaxivity with an R_2 value of 42.5 $s^{-1}mM^{-1}$, despite a slightly larger core diameter (~7.5 nm).[33] A decrease in core diameter is typically associated with decreased magnetic susceptibility due to the increased surface-area-to-volume ratio and the associated surface defects mentioned earlier. The drastic increase in relaxivity of catechol capped IOCCP-PEI and IOCCP as compared to IOCP demonstrates the catechol capping effect on the MR contrast enhancement capabilities of SPIONs.

IOCCP-PEI/DNA complex optimization

Gene delivery vectors must be able to efficiently condense DNA and maintain adequate size to traverse physiological barriers and reach target cells.[6] Additionally, adequate cationic surface charge is needed to aid in cell binding and facilitate the proton sponge effect to encourage endosomal escape after cellular internalization.[34] SPION/DNA complexes at ratios (w/w) of 0, 2, 5, 10, and 20 to 1, SPION to red fluorescent protein encoding plasmid DNA (pRFP) were evaluated for their hydrodynamic size and ζ potential (Figure S6, Supporting Information). SPION/DNA complexed at a ratio of 10:1 produced the best combination of size (hydrodynamic size = 54.3 nm) and cationic surface charge (ζ potential = 16.2 mV) and were further evaluated *in vitro*. Cell toxicity was observed in pilot transfection studies using IOCCP-PEI at a 10:1 SPION/DNA ratio, consequently, IOCCP was further PEGylated (IOCCP-PEI-PEG) with amine reactive 12 unit PEG (SMPEG12) at a 1:200 molar ratio of SPION to PEG to reduce charge and mitigate charge-induced toxicity.[35] The hydrodynamic size was not changed after the addition of PEG (54 nm) but the ζ potential was reduced slightly to 14.9 mV.

In vitro evaluation of SPION complexed with pRFP DNA

SF767 cells treated with IOCCP, IOCCP-PEI, and IOCCP-PEI-PEG complexed with DNA at a 10:1 ratio were evaluated at doses of 0.1, 0.5, 1, 2, 3, and 4 μg pRFP using the alamarBlue reagent to assess any reduction in cell metabolic activity (Figure 6a). The results were normalized as a % of control cells to determine cell viability. To compare with commercially available and commonly used transfection agents, Lipofectamine and 25 kDa PEI were used as positive controls. Lipofectamine was complexed at the manufacturer's suggested ratio of 3:1 Lipofectamine to DNA, while PEI was complexed at a 10:1 ratio consistent with the SPION complexes. IOCCP showed no toxicity at all evaluated pRFP doses, which was expected given the lack of high cationic charge and subsequent modest ζ potential (5.8 mV). Lipofectamine complexes maintained high cell viability at dosages of 0.1 and 0.5 μg pRFP (97.4 ± 7.5 % and 91.7 ± 7.3 %, respectively) but showed significant toxicity at an elevated dosage of 4 μg pRFP (17.4% ± 2.6%). PEI was far more toxic exhibiting a cell viability of 72.9 ± 3.8 % at a dosage of 0.1 μg pRFP and 11.7 ± 0.8 % at a dosage of 4 μg pRFP. IOCCP-PEI exhibited similar cell viability to PEI at low dosages (69.5 ± 4.3 %, 0.1 μg pRFP), but maintained better cell viability with increased DNA dose (35.4 ± 2.9 %, 4 μg pRFP). The PEG modification to IOCCP-PEI-PEG mitigated toxicity, increasing viability from 69.5 ± 4.3 % to 85.5 ± 3.5 % at 0.1 μg pRFP and from 35.4 ± 2.9 % to 56.3 ± 7.1 % at 4 μg pRFP.

The transfection capabilities of IOCCP, IOCCP-PEI, and IOCCP-PEI-PEG were evaluated using RFP expression in SF767 cells and analyzed by flow cytometry (Figure 6b). Pilot transfection and cell viability experiments indicated that a dose of 1 μg DNA/mL provided the best balance of transfection efficiency (Figure S7 in Supporting Information) and toxicity for the evaluated complexes. IOCCP-PEI had the highest transfection efficiency with 93.4 ± 0.9 % of cells positive for RFP expression, followed by IOCCP-PEI-PEG (91.7 ± 0.5 %) and Lipofectamine (78.1 ± 3.6 %) as shown in the representative histogram overlays (Figure 6b). To visualize RFP transfection of SF767 cells by IOCCP-PEI-PEG, cells were seeded on cover slips 24 h prior to 48 h incubation with SPIONs, nuclear stained (Dapi, blue), membrane stained (WGA-AF647, green) and evaluated by confocal fluorescence microscopy imaging (Figure 6c). IOCCP-PEI-PEG provides exceptional transfection efficiency with minimal toxicity as compared to PEI and commercially available Lipotectamine demonstrating potential as a gene delivery vector.

CONCLUSIONS

In summary, the synthesis of multi-dentate catechol modified CP and CCP further modified with PEI permitted a rapid synthesis/coating/functionalization of theranostic SPIONs capable of efficient gene transfection. The sonochemical synthesis method facilitated rapid production of superparamagnetic iron oxide cores with diameters of ~5.3 nm in the presence of CCP capping polymer. The modular approach allowed for fine-tuning of physiochemical properties by simply changing feed ratios of polymer constructs. The optimized PEI modified SPIONs displayed proper size and surface charge to navigate physiological barriers and successfully bind DNA. Catechol capping of the iron oxide surface lead to improved MR contrast enhancement over similar polymer coated SPIONs, demonstrating the potential utility of this SPION in real-time monitoring of gene delivery. Importantly, DNA loaded IOCCP-PEIs had excellent transfection efficiency *in vitro* and further modification with PEG greatly reduced toxicity without significantly hindering transfection efficiency. Extrapolation of this synthesis approach by replacing PEI with therapeutics and/or targeting functionalities would allow for rapid production of customizable theranostic agents tailored to individual patient needs.

Supplementary Material

Refer to Web version on PubMed Central for supplementary material.

ACKNOWLEDGEMENTS

This work is supported by NIH grants R01CA161953, R01CA134213. Z. Stephen acknowledge support through NCI training grant T32CA138312. We acknowledge lab assistance from H. Winter, J. White, and the use of resources at the Department of Pathologies cell analysis facility at University of Washington.

REFERENCES

1. Chen Q, Ke HT, Dai ZF, Liu Z. Nanoscale Theranostics for Physical Stimulus-Responsive Cancer Therapies. Biomaterials. 2015; 73:214–230. [PubMed: 26410788]
2. Kievit FM, Zhang M. Surface Engineering of Iron Oxide Nanoparticles for Targeted Cancer Therapy. Acc Chem Res. 2011; 44(10):853–862. [PubMed: 21528865]

3. Laurent S, Saei AA, Behzadi S, Panahifar A, Mahmoudi M. Superparamagnetic Iron Oxide Nanoparticles for Delivery of Therapeutic Agents: Opportunities and Challenges. Expert Opin. Drug Deliv. 2014; 11(9):1449–1470. [PubMed: 24870351]
4. Stephen ZR, Kievit FM, Zhang MQ. Magnetite Nanoparticles for Medical Mr Imaging. Mater. Today. 2011; 14(7–8):330–338.
5. Thomas R, Park IK, Jeong YY. Magnetic Iron Oxide Nanoparticles for Multimodal Imaging and Therapy of Cancer. Int. J. Mol. Sci. 2013; 14(8):15910–15930. [PubMed: 23912234]
6. Kievit FM, Zhang M. Cancer Nanotheranostics: Improving Imaging and Therapy by Targeted Delivery across Biological Barriers. Advanced materials. 2011; 23(36):H217–247. [PubMed: 21842473]
7. Kievit FM, Zhang MQ. Surface Engineering of Iron Oxide Nanoparticies for Targeted Cancer Therapy. Acc Chem Res. 2011; 44(10):853–862. [PubMed: 21528865]
8. Korringa J, Seevers DO, Torrey HC. Theory of Spin Pumping and Relaxation in Systems with a Low Concentration of Electron Spin Resonance Centers. Physical Review. 1962; 127(4):1143. &.
9. Hermanson, GT. Bioconjugate Techniques. 2nd ed. Elsevier Inc; Oxford UK: 2008.
10. Karpishin TB, Gebhard MS, Solomon EI, Raymond KN. Spectroscopic Studies of the Electronic-Structure of Iron(Iii) Tris(Catecholates). Journal of the American Chemical Society. 1991; 113(8): 2977–2984.
11. Amstad E, Gillich T, Bilecka I, Textor M, Reimhult E. Ultrastable Iron Oxide Nanoparticle Colloidal Suspensions Using Dispersants with Catechol-Derived Anchor Groups. Nano Letters. 2009; 9(12):4042–4048. [PubMed: 19835370]
12. Coxon TP, Fallows TW, Gough JE, Webb SJ. A Versatile Approach Towards Multivalent Saccharide Displays on Magnetic Nanoparticles and Phospholipid Vesicles. Org. Biomol. Chem. 2015; 13(43):10751–10761. [PubMed: 26360423]
13. Mondini S, Drago C, Ferretti AM, Puglisi A, Ponti A. Colloidal Stability of Iron Oxide Nanocrystals Coated with a Peg-Based Tetra-Catechol Surfactant. Nanotechnology. 2013; 24(10)
14. Sasikala ARK, GhavamiNejad A, Unnithan AR, Thomas RG, Moon M, Jeong YY, Park CH, Kim CS. A Smart Magnetic Nanoplatform for Synergistic Anticancer Therapy: Manoeuvring Mussel-Inspired Functional Magnetic Nanoparticles for Ph Responsive Anticancer Drug Delivery and Hyperthermia. Nanoscale. 2015; 7(43):18119–18128. [PubMed: 26471016]
15. Saville SL, Stone RC, Qi B, Mefford OT. Investigation of the Stability of Magnetite Nanoparticles Functionalized with Catechol Based Ligands in Biological Media. Journal of Materials Chemistry. 2012; 22(47):24909–24917.
16. Wei H, Insin N, Lee J, Han HS, Cordero JM, Liu WH, Bawendi MG. Compact Zwitterion-Coated Iron Oxide Nanoparticles for Biological Applications. Nano Letters. 2012; 12(1):22–25. [PubMed: 22185195]
17. Dolores R, Raquel S, Adianez GL. Sonochemical Synthesis of Iron Oxide Nanoparticles Loaded with Folate and Cisplatin: Effect of Ultrasonic Frequency. Ultrason. Sonochem. 2015; 23:391–398. [PubMed: 25218767]
18. Sodipo BK, Aziz AA. A Sonochemical Approach to the Direct Surface Functionalization of Superparamagnetic Iron Oxide Nanoparticles with (3-Aminopropyl)Triethoxysilane. Beilstein Journal of Nanotechnology. 2014; 5:1472–1476. [PubMed: 25247130]
19. Ashokkumar M, Lee J, Kentish S, Grieser F. Bubbles in an Acoustic Field: An Overview. Ultrason. Sonochem. 2007; 14(4):470–475. [PubMed: 17234444]
20. Kievit FM, Veiseh O, Bhattarai N, Fang C, Gunn JW, Lee D, Ellenbogen RG, Olson JM, Zhang MQ. Pei-Peg-Chitosan-Copolymer-Coated Iron Oxide Nanoparticles for Safe Gene Delivery: Synthesis, Complexation, and Transfection. Adv. Funct. Mater. 2009; 19(14):2244–2251. [PubMed: 20160995]
21. Na HB, Palui G, Rosenberg JT, Ji X, Grant SC, Mattoussi H. Multidentate Catechol-Based Polyethylene Glycol Oligomers Provide Enhanced Stability and Biocompatibility to Iron Oxide Nanoparticies. Acs Nano. 2012; 6(1):389–399. [PubMed: 22176202]
22. Smolensky ED, Park HYE, Berquo TS, Pierre VC. Surface Functionalization of Magnetic Iron Oxide Nanoparticles for Mri Applications - Effect of Anchoring Group and Ligand Exchange Protocol. Contrast Media Mol. Imaging. 2011; 6(4):189–199. [PubMed: 21861279]

23. Kievit FM, Veiseh O, Fang C, Bhattarai N, Lee D, Ellenbogen RG, Zhang MQ. Chlorotoxin Labeled Magnetic Nanovectors for Targeted Gene Delivery to Glioma. Acs Nano. 2010; 4(8): 4587–4594. [PubMed: 20731441]
24. Faure A-C, Dufort S, Josserand V, Perriat P, Coll J-L, Roux S, Tillement O. Control of the in Vivo Biodistribution of Hybrid Nanoparticles with Different Poly(Ethylene Glycol) Coatings. Small. 2009; 5(22):2565–2575. [PubMed: 19768700]
25. Longmire M, Choyke PL, Kobayashi H. Clearance Properties of Nano-Sized Particles and Molecules as Imaging Agents: Considerations and Caveats. Nanomedicine. 2008; 3(5):703–717. [PubMed: 18817471]
26. Cornell, RM.; Schwertmann, U. The Iron Oxides: Structure, Properties, Reactions, Occurrences and Uses. 2nd ed. Wiley-VCH; New York: 2003. p. 703
27. Saraswathy A, Nazeer SS, Jeevan M, Nimi N, Arumugam S, Harikrishnan VS, Varma PRH, Jayasree RS. Citrate Coated Iron Oxide Nanoparticles with Enhanced Relaxivity for in Vivo Magnetic Resonance Imaging of Liver Fibrosis. Colloid Surf. B-Biointerfaces. 2014; 117:216–224.
28. Saraswathy A, Nazeer SS, Nimi N, Arumugam S, Shenoy SJ, Jayasree RS. Synthesis and Characterization of Dextran Stabilized Superparamagnetic Iron Oxide Nanoparticles for in Vivo Mr Imaging of Liver Fibrosis. Carbohydr. Polym. 2014; 101:760–768. [PubMed: 24299836]
29. Yuen AKL, Hutton GA, Masters AF, Maschmeyer T. The Interplay of Catechol Ligands with Nanoparticulate Iron Oxides. Dalton Transactions. 2012; 41(9):2545–2559. [PubMed: 22241454]
30. Borges RP, Guichard W, Lunney JG, Coey JMD, Ott F. Magnetic and Electric “Dead” Layers in (La0.7sr0.3)Mno3 Thin Films. J. Appl. Phys. 2001; 89(7):3868–3873.
31. Oguz K, Jivrajka P, Venkatesan M, Feng G, Coey JMD. Magnetic Dead Layers in Sputtered Co(40)Fe(40)B(20) Films. J. Appl. Phys. 2008; 103(7):3.
32. Nagesha DK, Plouffe BD, Phan M, Lewis LH, Sridhar S, Murthy SK. Functionalization-Induced Improvement in Magnetic Properties of Fe3o4 Nanoparticles for Biomedical Applications. J. Appl. Phys. 2009; 105(7):3.
33. Stephen ZR, Kievit FM, Veiseh O, Chiarelli PA, Fang C, Wang K, Hatzinger SJ, Ellenbogen RG, Silber JR, Zhang M. Redox-Responsive Magnetic Nanoparticle for Targeted Convection-Enhanced Delivery of O6-Benzylguanine to Brain Tumors. ACS Nano. 2014; 8(10):10383–10395. [PubMed: 25247850]
34. Behr JP. The Proton Sponge: A Trick to Enter Cells the Viruses Did Not Exploit. Chimia. 1997; 51(1–2):34–36.
35. Takae S, Miyata K, Oba M, Ishii T, Nishiyama N, Itaka K, Yamasaki Y, Koyama H, Kataoka K. Peg-Detachable Polyplex Micelles Based on Disulfide-Linked Block Catiomers as Bioresponsive Nonviral Gene Vectors. Journal of the American Chemical Society. 2008; 130(18):6001–6009. [PubMed: 18396871]

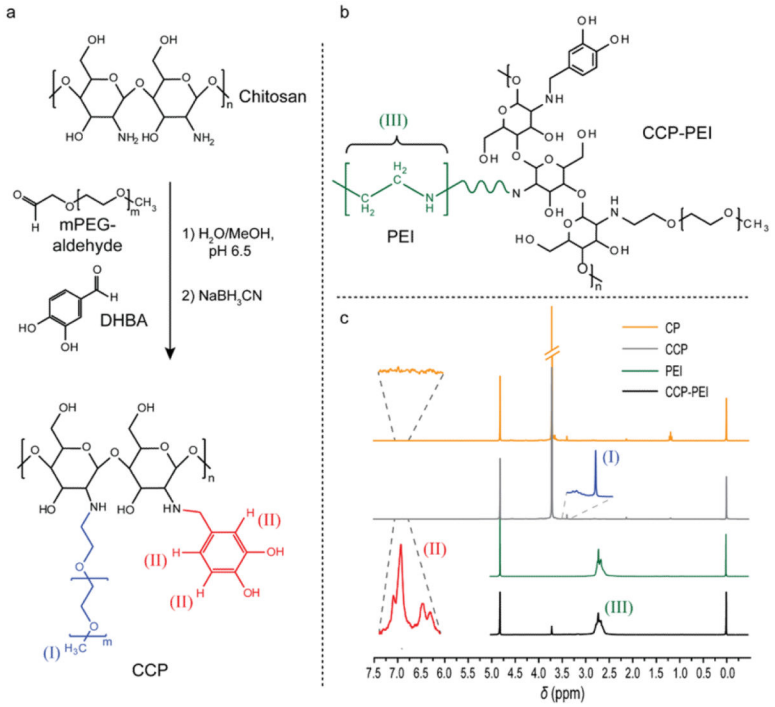

Figure 1.

Synthesis and characterization of CCP and CCP-PEI. a) CCP synthesis *via* catechol and PEG modification of low molecular weight chitosan by reductive amination. b) Chemical structure of CCP-PEI and its characteristic ethylenimine group. c) Proton NMR analysis of CCP and CCP-PEI. The methoxy hydrogens of PEG (I) and the aromatic catechol hydrogens (II) were used to determine the extent of grafting on the chitosan backbone. Characteristic peaks associated with the ethylenimine group of PEI (III) confirm the presence of PEI on IOCCP-PEI. All samples were analyzed in D_2O in the presence of TSP.

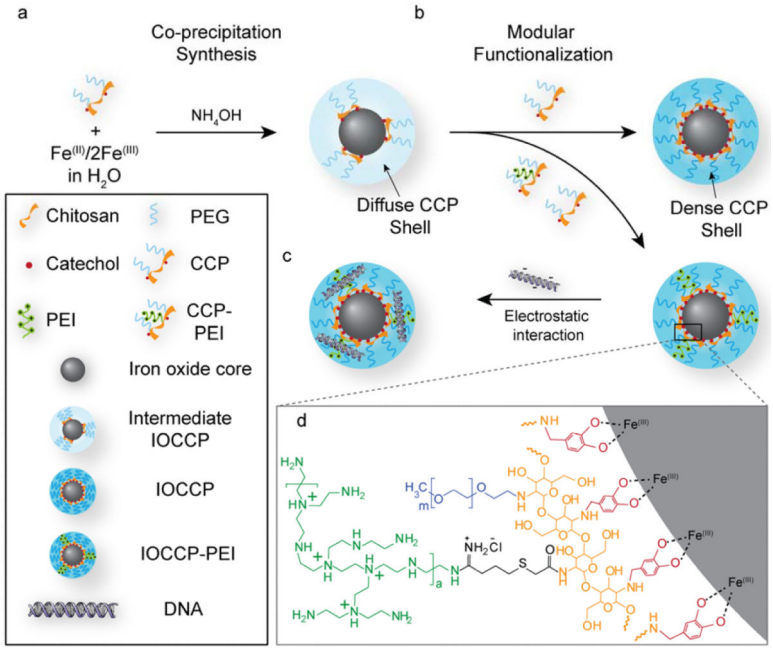

Figure 2.

Synthesis and modular functionalization of IOCCP and IOCCP-PEI. a) Diffusely coated intermediate IOCCPs were initially synthesized in the presence of a low concentration of CCP then (b) supplemented with additional polymer (CCP or CCP-PEI) to add functionality to the SPION and increase coating density. c) PEI functionalized SPIONs bind DNA through electrostatic interactions. d) Chemical detail of the SPION surface and catechol-polymer interface.

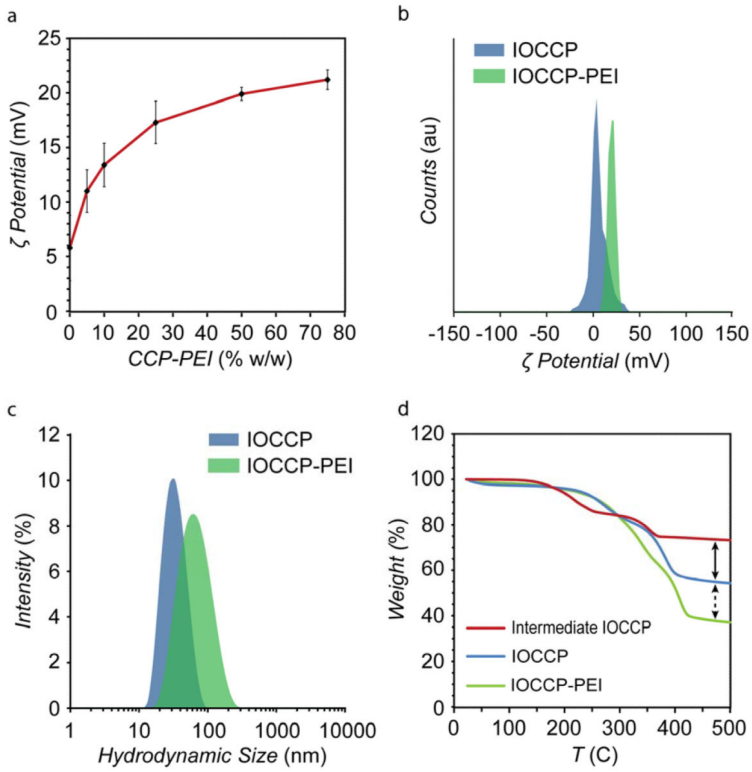

Figure 3.

Characterization of size and surface properties of IOCCP and IOCCP-PEI. a) Evaluation of change in weight % CCP-PEI on ζ potential of IOCCP-PEI. The mean ζ potential for each ratio was determined from three separate batches of IOCCP-PEI. Error bars = standard deviation. b) ζ potential distributions of IOCCP (blue) and IOCCP-PEI (green) in 20mM HEPES, pH 7.4. c) Intensity based hydrodynamic size distributions of IOCCP (blue) and IOCCP-PEI (green) in 20mM HEPES, pH 7.4. d) TGA analysis showing increased polymer density for IOCCP and IOCCP-PEI (50% CCP-PEI w/w) as compared to intermediate IOCCPs.

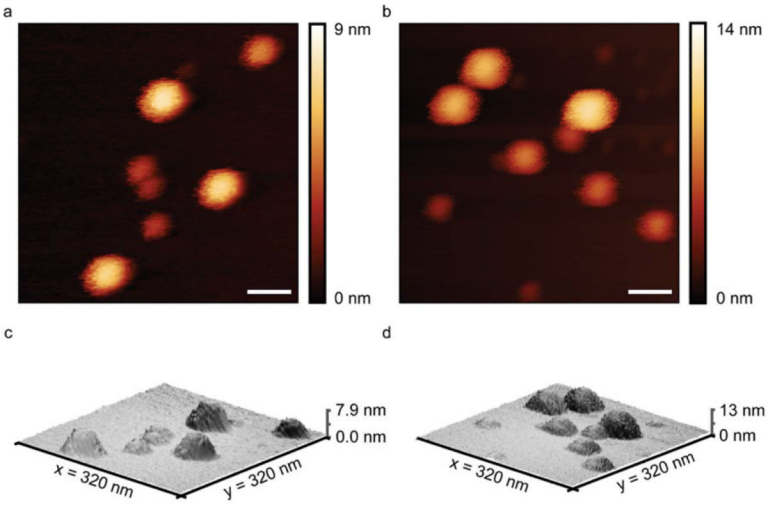

Figure 4.

AFM images of IOCCP and IOCCP-PEI acquired in tapping mode. 2D color maps of (a) IOCCP and (b) IOCCP-PEI and corresponding 3D topography maps of (c) IOCCP and (d) IOCCP-PEI. Scale bar corresponds to 50 nm.

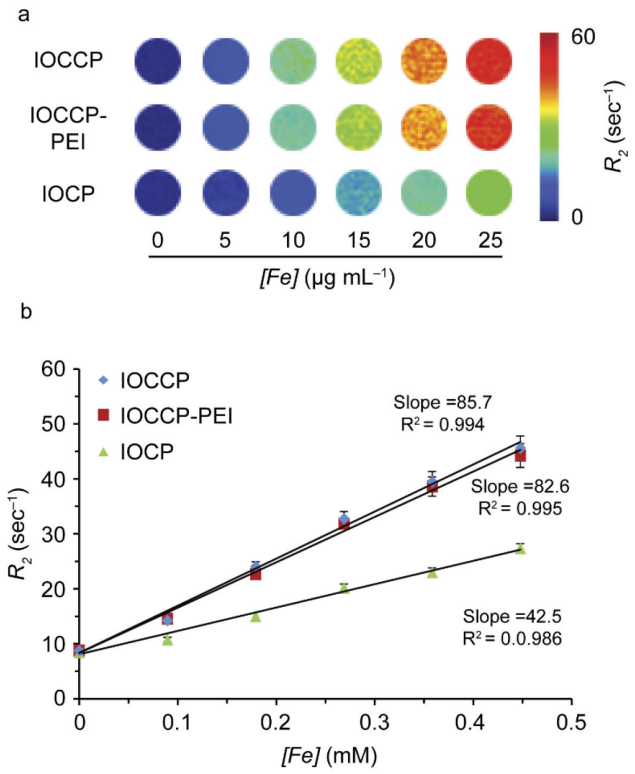

Figure 5.

Characterization of MR relaxation properties for IOCCP-PEI and IOCCP. a) Colorized R_2 maps of phantoms of IOCCP, IOCCP-PEI and IOCP at various iron concentrations. b) Magnetic R_2 relaxivity of IOCCP, IOCCP-PEI and IOCP was calculated to be 85.7, 82.6 and 42.5 $s^{-1}mM^{-1}$, respectively, at 14 T field strength.

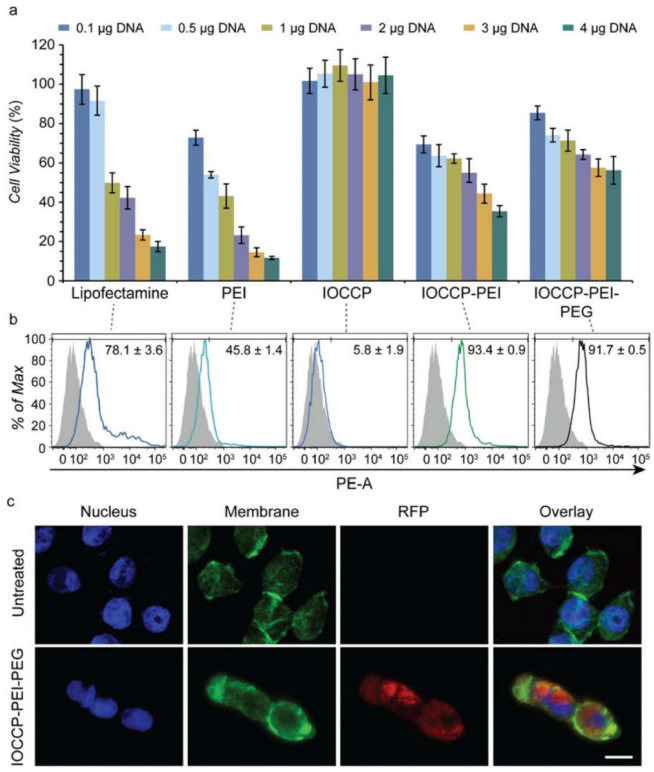

Figure 6.

Assessment of cell viability and transfection efficiency in SF767 cells (a) Evaluation of cytotoxicity by the alamarBlue assay after 48 h incubation with 0.1, 0.5, 1, 2, 3, or 4 μg of pRFP. IOCCP, IOCCP-PEI, IOCCP-PEI-PEG, and PEI were complexed at a 10:1 w/w ratio of DNA to transfection agent and Lipofectamine was complexed at a 3:1 w/w ratio. b) Representative histogram overlays of untreated SF767 cells compared with Lipofectamine, PEI, IOCCP, IOCCP-PEI, and IOCCP-PEI transfected cells at a dose of 1 μg pRFP. c) Confocal fluorescence microscopy imaging of untreated SF767 cells and SF767 cells treated with 1 μg pRFP complexed with IOCCP-PEI-PEG. The DAPI nuclear stain is shown in blue, the WGA-AF647 membrane stain is shown in green and RFP expression is shown in red. The scale bar corresponds to 10 μm. 5000 cells analyzed; error bars indicate ± standard deviation.